phys. stat. sol. (RRL) **2**, No. 3, 132–134 (2008) / **DOI** 10.1002/pssr.200802076

pss +++rapid research letters+++
www.pss-rapid.com

# Synthesis and catalytic activity of hybrid metal/silicon nanocomposites

**Sergej Polisski[*,1], Bernhard Goller[1], Alexei Lapkin[2], Simon Fairclough[1], and Dmitry Kovalev[1]**

[1] Department of Physics, University of Bath, Claverton Down, Bath BA2 7AY, United Kingdom
[2] Department of Chemical Engineering, University of Bath, Claverton Down, Bath BA2 7AY, United Kingdom

Received 17 March 2008, revised 21 April 2008, accepted 21 April 2008
Published online 23 April 2008

**PACS** 61.46.Hk, 68.37.Og, 73.20.Mf, 81.07.–b, 82.65.+r

* Corresponding author: e-mail s.polisski@bath.ac.uk, Phone: +44 1225 383113, Fax: +44 1225 38 5118

In this Letter we demonstrate that hydrogen-terminated porous silicon (PSi) layers and powders can serve as highly efficient reductive templates for noble metal salts. The reduction results in metal nanoparticle (NP) formation in the pores of PSi. Gold NP formation has been monitored *in-situ* by measuring the plasmon resonance response. Pt NPs, formed in the PSi matrix, were investigated by transmission electron microscopy and energy-dispersive X-ray analysis. Furthermore, hybrid Pt/PSi nanocomposites exhibit a high catalytic activity for CO oxidation.

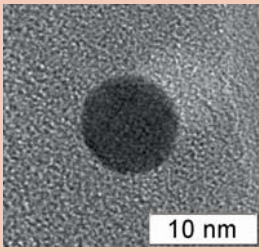


HRTEM image of a Pt nanoparticle reduced inside the PSi matrix. Platinum lattice fringes $d_{\langle 111\rangle} = 2.27$ Å can be seen.



**1 Introduction** Porous silicon (PSi) nanostructures, prepared either by electrochemical or stain etching processes exhibit a very large (up to 500 $m^2/cm^3$) hydrogenated internal surface area [1]. We demonstrate that these morphological properties result in a high reductive potential of its internal surface due to hydrogen termination. Coulthard and co-workers have shown that noble metal salts, dissolved in water can be reduced on the surface of PSi layers [2]. However, the hydrogenated PSi surfaces are hydrophobic [1], and therefore, the large internal surface area of PSi was not accessible to metal salts and hence not exploited. In recent years the catalysis based on metal NPs has been widely developed [3]. Scaled to nanosizes, metal particles are more efficient in catalysis due to the large extended surface area and exposed higher energetic surfaces. They promote chemical reactions which cannot be realized otherwise, because of the new provided reaction sites and modified surface properties [4]. Nanoparticles are not only competing, but frequently replacing up to date known homo- and heterogeneous catalysts [5].

The reactive PSi templates open promising possibilities for applications in nano metal-supported catalysis. Salts of Pt and Au were reduced on the internal Si nanocrystalline surface. The obtained metal nanoparticles are in the size range of 3 nm to 20 nm. Hydrogen effusion experiments show that Si surfaces lacking hydrogen termination are not able to act as a reductive template. This fact underlines the crucial difference for metal NP formation between H-terminated PSi and widely used chemically inactive templates.

The catalytic activity of the developed nanocomposites has been studied using a conversion of carbon monoxide (CO) to $CO_2$ in oxygen.

## 2 Experimental

### 2.1 Sample preparation and characterization

Free-standing PSi layers have been prepared via standard electrochemical etching of B-doped (100)Si substrates with a typical resistivity of 2–5 Ω cm (microporous Si, ~70% porosity) [1]. To prepare nanocrystalline PSi powder we used metallurgical grade powder having a mean particle size of 4 μm. The stain etching was performed as described elsewhere [6]. The internal surface area of the PSi was evaluated from the adsorption–desorption iso-

therm of nitrogen at 77 K (BET) [7]. The pore size distribution was calculated by BJH method [8].

Metal salts were dissolved in ethanol. Then, PSi was immersed into the metal salt solutions at different temperatures. For the characterisation of the sample morphology, high resolution transmission electron microscopy measurements (HRTEM) of as-prepared PSi samples and metal/PSi (M/PSi) nanocomposites were performed using a JEM-2010 (JEOL) apparatus operated at 200 kV.

For plasma resonance experiments we used electrochemically etched PSi layers. These PSi samples were inserted in a quartz cuvette, containing solutions of Au salts in ethanol (100, 10, 1 and 0.1 mM). Optical transmission spectra were then taken at regular time intervals of both the solution and the PSi samples.

**2.2 Catalytic activity measurements** The catalytic activity of the metal NPs, embedded in the PSi matrix, was tested using the oxidation reaction of carbon monoxide in the absence of water and hydrogen. For this purpose a gas mixture of 1% CO/20% $O_2$, balanced in helium, was used providing a gas flow of 75 $cm^3$ $min^{-1}$ through a quartz microreactor. In all experiments a mixture of catalyst sample with 40 wt% of quartz particles (10 μm) were used to assure homogeneous gas flow distribution. The actual amount of used metal was measured to determine its catalytic activity. The reaction was monitored by a gas-sampling mass spectrometer to trace the $CO_2$ output.

## 3 Results and discussion

**3.1 Morphology of PSi powder and M/PSi nanocomposites** As confirmed by our HRTEM measurements the stain etching of p-doped (Al) polycrystalline Si powder results in a sponge-like structure that consists of Si nanocrystals and pores in the nanometre range. To obtain the surface area and the pore size distribution of an as-prepared PSi powder, adsorption–desorption isotherm was measured. The surface area of 160 $m^2/g$ and a mean pore size of 7 nm (coincides well with HRTEM images) were derived from the $N_2$ desorption isotherm. We identified Si–H, Si–$H_2$ and Si–$H_3$ bonds as the dominating surface groups using infrared absorption spectroscopy.

To demonstrate the importance of hydrogen surface termination for NP formation we performed hydrogen effusion experiments by heating the samples to 400 °C. Afterwards a metal salt reduction was performed to compare both, an as-prepared and a thermally treated sample. While for H-terminated samples efficient metal NP formation was observed, no reductive activity was noticed for the second type of samples under the same conditions. Therefore, surface Si–$H_x$ groups act as conjugate couples for the reduction of metal salts in the PSi matrix. We found that the pore size of the PSi support, metal formation temperature and metal salt concentration are crucial in defining the overall morphology of the nanocomposites. HRTEM image of Pt NPs, formed in the PSi matrix, is shown in Fig. 1. The mean particle size of Pt NPs determined by HRTEM

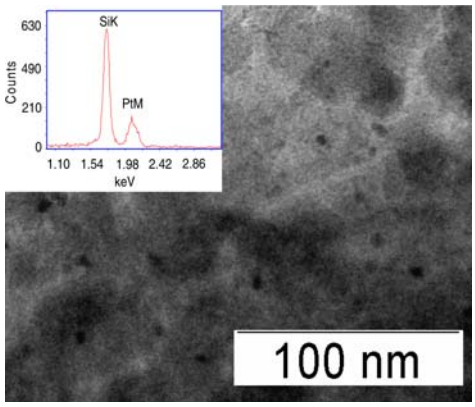


**Figure 1** (online colour at: www.pss-rapid.com) HRTEM image of a Pt/PSi hybrid nanocomposite. Pt loading is 1 wt% with respect to PSi support. Inset: EDX analysis showing Si K and Pt M peaks, respectively.

technique is around 6–8 nm, which coincides with the average pore size. This evidences the pre-definition of the size of NPs by the pore size of the support.

In Fig. 1 several Pt nanoparticles of similar size can be seen. The energy-dispersive X-ray (EDX) analysis, obtained from metal NP in this area of the sample, underlines the presence of bulk Pt in the PSi matrix.

**3.2 In-situ plasma resonance monitoring of metal NP's formation** To study Au NP formation *in-situ*, thin (up to 25 μm) free standing layers of PSi with pore sizes of 5–10 nm were employed. Time-dependent NP formation inside PSi matrix was studied by measuring the metal plasma oscillation frequency response with time. The plasma frequency of metal particles is dependent on their shape, size and the surrounding dielectric medium [9].

The area under extinction spectra rises linearly with time during the first hour of the reaction (inset of Fig. 2).

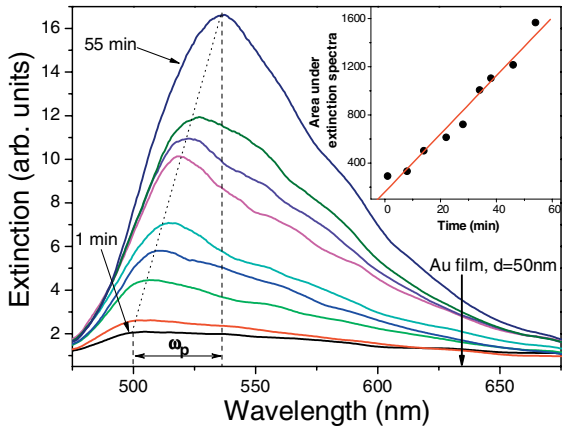


**Figure 2** (online colour at: www.pss-rapid.com) In-situ monitored plasma frequency of formed Au NPs. 0.1 mM concentrated $HAuCl_4$ solution was used. Extinction spectra were recorded in periodic steps. Inset: Area under the extinction spectra versus time. The dotted lines are only for eye guidance.

Only after two hours the extinction spectra reach the steady state.

Nevertheless, even after two hours the plasmon frequency of the formed NPs (580 nm) is still far from the bulk value (634 nm, [10]), indicated by the arrow in Fig. 2. For Au NPs it is in the visible range ($\lambda = 550$ nm). Pt has its plasmon resonance in the UV-range (~235 nm) [11], which makes the optical studies of Pt NP formation in PSi impossible, as PSi adsorbs very efficiently in this range.

Plasmon resonance is a fingerprint of Au NP formation. We assume that the amplitude of the integral area under the extinction spectra scales in the first approximation with the quantity of reduced particles. At concentrations above 10 mM the formation of micrometer-large particles has been detected. At lower concentrations gold particles are formed much slower inside PSi template. The plasmon resonance of gold shifts only slightly to longer wavelengths with time, implying a nanometer particle size (Fig. 2). The area under extinction spectra rises linearly with time during the first hour of the reaction, showing that a uniform formation of small particles can be realized (inset of Fig. 2).

### 3.3 Catalytic activity of Pt/PSi nanocomposites

Pt/PSi hybrid nanocomposites were tested in CO oxidation reaction. Figure 3 shows a sharp step in CO conversion efficiency when the light-off temperature ($T_L$) is reached. A complete conversion was achieved for all Pt loadings (Fig. 3). A Pt-free sample as expected showed no activity (circles, Fig. 3) over the whole reaction temperature range of interest. A negligible conversion of CO was registered above 300 °C; this probably results from hydrogen desorption, which takes place in the temperature range of 350 °C to 500 °C. Due to the presence of dangling bonds in the peripheral PSi sites, small amount of CO and $O_2$ molecules can be adsorbed at the active sites and react to the final product: carbon dioxide.

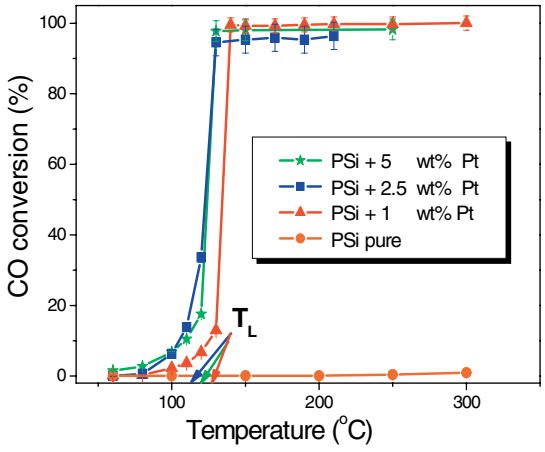


**Figure 3** (online colour at: www.pss-rapid.com) CO conversion by Pt/PSi nanocomposites. Gas flow rate is 75 $cm^3$/min, mass of catalyst used 350 mg. Light-off temperatures ($T_L$) are indicated by arrows.

Since almost no difference in catalytic activity for all Pt loaded samples has been found, we believe that similar reaction sites are involved due to an equivalent particle size distribution.

**4 Conclusions** Several key features make PSi matrix different from other known support materials for catalysis: high chemical reactivity of extended H-terminated surface and tuneable pore size. Furthermore, an undulating pore morphology prevents agglomeration of formed NPs and their leakage from PSi matrix.

Plasma resonance experiments seem to be a powerful tool to investigate NP formation *in-situ*. Using this technique a controllable synthesis of NPs can be realized. We found that the NP formation is strongly dependent on the metal salt concentration and the exposure time.

The CO oxidation experiments provide evidence for the high catalytic activity of platinum NPs embedded in PSi matrix. The conversion efficiency is found to be dependent on the gas flow rate, salt concentration, metal particle size and the pore size distribution. We assume that an optimized catalyst based on Pt/PSi nanocomposites will need even smaller metal loadings.

**Acknowledgements** S.P. wishes to thank his father for faith and support. This work was in part supported by Vesta Ceramics and Engineering and Physical Sciences Research Council via grant EP/E012183/1.

## References

[1] A. G. Cullis, L. T. Canham, and P. D. J. Calcott, J. Appl. Phys. **82**, 909 (1997).
[2] I. Coulthard and T. K. Sham, Solid State Commun. **105**, 751 (1998).
[3] D. Astruc, F. Lu, and R. Aranzaes Jaime, Angew. Chem., Int. Ed. **44**, 7852 (2005).
[4] A. S. K. Hashmi and J. Hutchings Graham, Angew. Chem., Int. Ed. **45**, 7896 (2006).
[5] G. P. Chiusoli and P. M. Maitlis (eds.), Metal-Catalysis in Industrial Organic Processes (RSC Publishing, Cambridge, 2006).
[6] S. Limaye et al., phys. stat. sol. (a) **204**, 1297 (2007).
[7] S. Brunauer, P. H. Emmett, and E. Teller, J. Am. Chem. Soc. **60**, 309 (1938).
[8] E. P. Barrett, L. G. Joyner, and P. P. Halenda, J. Am. Chem. Soc. **73**, 373 (1951).
[9] S. A. Maier, Plasmonics: Fundamentals and Applications (Springer Science + Business Media LLC, New York, 2007).
[10] E. D. Palik, Handbook of Optical Constants of Solids (Academic Press, New York, 1985), p. 804.
[11] S. Remita et al., Radiat. Phys. Chem. **54**, 463 (1999).